PROCEEDINGS A

rspa.royalsocietypublishing.org

Research

Cite this article: Deane JHB, Bevan JJ. 2018 A hydrostatic model of the Wirtz pump. *Proc. R. Soc. A* **474**: 20170533.
http://dx.doi.org/10.1098/rspa.2017.0533

Received: 2 August 2017
Accepted: 23 February 2018

Subject Areas:
mathematical modelling

Keywords:
Wirtz pump, water-powered pump, alternative technology, hydrostatics, dynamical systems, optimization

Author for correspondence:
Jonathan H. B. Deane
e-mail: j.deane@surrey.ac.uk

A hydrostatic model of the Wirtz pump

Jonathan H. B. Deane and Jonathan J. Bevan

Department of Mathematics, University of Surrey, Guildford GU2 7XH, UK

JHBD, 0000-0003-1088-712X

The Wirtz pump is not only an excellent example of alternative technology, using as it does the kinetic energy of a stream to raise a proportion of its water, but its mathematical modelling also poses several intriguing problems. We give some history of the Wirtz pump and describe its operation. Taking a novel dynamical systems approach, we then derive a discrete mathematical model in the form of a mapping that describes its hydrostatic behaviour. Our model enables us to explain several aspects of the behaviour of the pump as well as to design one that gives approximately maximal, and maximally constant, output pressure.

1. Introduction

A first encounter with the Wirtz pump can hardly fail to impress: essentially, a rotating spiral of pipe, mounted in a vertical plane and arranged so that one open end dips below the surface of a reservoir of water once per revolution, easily adapted to be driven by water power, can be used to pump a useful quantity of water to a height of several metres. The pump requires only one critical component, a rotating coupling, which connects a turning pipe to a stationary one aligned along the same axis, in a watertight, low-friction manner. The first author came across an account of this 1746 invention of H. Andreas Wirtz, a Zurich pewterer, several years ago in [1], and was inspired to build one—the result can be seen in figure 1. Eight years later, this pump, which is attached to the spokes of a waterwheel, is still providing reliable irrigation at a height of 5.5 m above a stream, at a rate of about 11 min^{-1}.

The pumps considered in the literature fall into two categories: helical pumps, in which the pipe is formed into a series of turns all of the same radius (the pipe may be imagined to be wound around a cylinder) and spiral pumps, an essentially planar arrangement in which the

THE ROYAL SOCIETY PUBLISHING

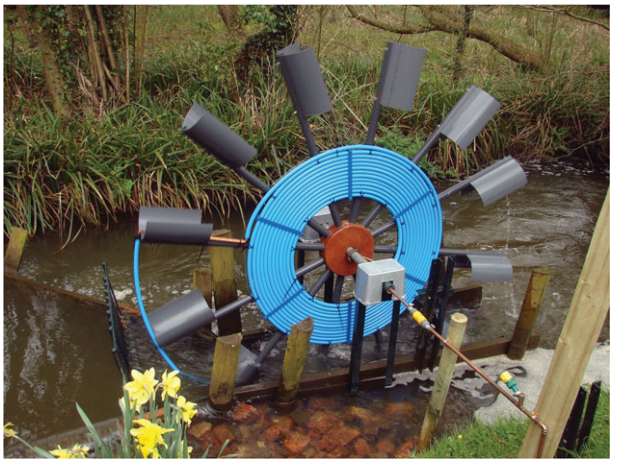

Figure 1. Practical Wirtz pump in the stream at the bottom of the first author's garden. The pump itself is the spiral of pipe, which has been attached to the spokes of an undershot waterwheel. The water flows from left to right and its speed is increased by the narrowing of the stream at this point. The rotating coupling can be seen in the horizontal copper pipe between the waterwheel and the short, round wooden post. (Online version in colour.)

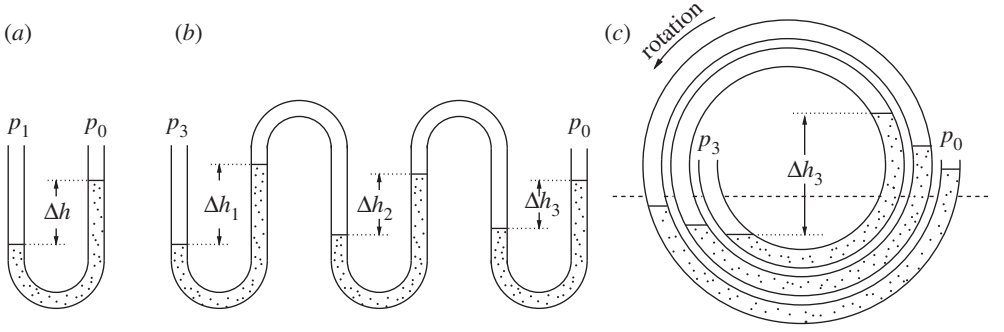

Figure 2. Operation of the spiral Wirtz pump. All three figures show sections of pipe containing water (dotted) and air. In (*a*), we have the simple manometer, and in (*b*), three such manometers connected in series. In (*c*), we show the same configuration as (*b*) but arranged as a three-turn Archimedean spiral—one in which the radius, ρ, varies linearly with angle ψ (i.e. in polar form, $\rho = k\psi$ with k constant). The spiral rotates anticlockwise and its open end, on the right, is sometimes submerged in the water whose surface is shown as a dashed horizontal line.

radius of successive turns decreases. Our main interest is to take a—we believe, novel—dynamical systems approach to modelling the spiral case, which we refer to as the Wirtz pump, because it is likely to resemble Wirtz's invention most closely. Other authors have used the terms 'spiral pump', 'coil pump' or 'manometric pump' to refer to both spiral and helical geometries.

We now give a pictorial explanation of how a rotating spiral of pipe can function as a pump. Figure 2 shows three configurations of pipe containing one or more 'plugs' of water. Figure 2*a* shows a U-tube manometer, the simplest pressure gauge, familiar from school physics. Pascal's Law, which we discuss in §2a, tells us that the pressure difference $p_1 - p_0$ is proportional to the height difference, Δh, between the surfaces of the water in the right and left limbs, respectively. Taking this idea further, figure 2*b* shows three such manometers connected in series, this arrangement giving an increased pressure difference, $p_3 - p_0$, proportional to $\Delta h_1 + \Delta h_2 + \Delta h_3$. Finally, in figure 2*c*, we imagine the previous configuration to be 'folded' around alternate vertical limbs, giving the spiral configuration shown, with $p_3 - p_0$ again being proportional to the sum of the height differences. In practice, the spiral would be likely to consist of many more than three turns.

We can see from the foregoing the importance of the alternation of plugs of air (a low-density fluid) with plugs of water (high-density fluid) to the working of the pump: it is the fact that the high-density fluid is displaced that generates pressure within the low-density fluid, and a spiral pipe can only be filled in this way if its open end is sometimes submersed in water, and sometimes in air. The horizontal dashed line in figure 2*c* shows a notional water level which imposes this filling pattern as the spiral rotates. As we shall see, the assumption that the plugs of water remain intact at all times is also necessary when it comes to modelling the pump.

Our main interest here is to devise a mathematical model of the hydrostatic behaviour of the Wirtz pump, and we take a dynamical systems approach. We first explain the assumptions under which our model of the pump is valid. The model itself turns out to be a two-dimensional, nonlinear map which relates the air pressure and the configuration of the plugs of water in two successive turns of the spiral. To write down the map, we need to consider carefully the computation of arc lengths of sections of helices and spirals; we suspect that one reason for the focus on helices in earlier literature is the extra computation needed in the spiral case. This leads to many of our results being numerical. We further explain (i) how the pump is self-regulating, that is, how, within limits, it will automatically produce the required output pressure; (ii) an approach to devising, approximately, a spiral that gives the maximum output pressure, subject to given constraints, which we name the 'quasi-optimal spiral' (QOS), and (iii) how to model 'air lift' in a simple case.

There is some early literature on the Wirtz pump. For instance, the study of Gregory [2] is a reference to the spiral, as opposed to the helical pump, which anticipates, by 200 years, several of the problems we consider here. The author not only addresses the question of the spiral that generates the maximum pressure, but also realizes the potential of air lift—a direct and useful consequence of the fact that the input to and output from the pump must consist of alternating plugs of air and water. The other early references, [3,4], add detail, and it is interesting to read of a water-powered Wirtz pump installed in Arkhangelsk in 1784, which [4] claims 'raised a hogshead of water in a minute to an elevation of seventy-four feet, and through a pipe seven hundred and sixty feet long'. These figures are impressive—a hogshead being 200–300 l, the power required just to raise this quantity of water with no friction would be at least 750 W.

More recent works [5–8] concentrate mostly on the helical pump. An experimental approach is taken in [5]. The helix is rotated at rates of up to 120 r.p.m., hence in this study, many different dynamical effects are likely to be important. The device is designed to be rotated by integral vanes, not by attachment to a waterwheel. The thesis [7] concentrates on both modelling the system and carrying out experiments. Interestingly, the adiabatic equation, $pv^\gamma = \text{const.}$ [9], is used to model the compression of air in the pump, rather than Boyle's Law [9]. Among much else, data are given on failure modes (for example, spillover, in which water in one turn of the helix spills over into the next turn; bubbling, in which air bubbles up through a plug of water; and blow-back, in which the system becomes unstable and water is forcibly ejected from the intake.) In [6], we find a summary of the main results in [7] as well as a brief treatment of air lift.

A different application is described in [8]. Both helical and spiral cases are briefly discussed, but Belcher's interest is in using the spiral pump concept for the removal of floating pollutants from the surface of the sea.

The website http://lurkertech.com/water/, where [1] can be found, is a mine of practical information and experimental and historical data relating to water-powered pumps. The Wirtz pump is dealt with from an experimental viewpoint in [1], which reports on the performance of a large experimental pump. There is also a link to a most instructive video [10] showing a helical pump built from translucent pipe, in which the positioning of the plugs of water can be seen. The pipe used in the video is about the same size as that used in figure 1.

The rest of the paper is organized as follows. In §2, we discuss the assumptions upon which our model is based, show how we estimate volumes of curved pipe, and give a table of realistic parameter values—'realistic' because they are taken from the pump shown in figure 1. In §3, we derive the two-dimensional map referred to above, in a form that is valid for a class of spirals. In §4, we introduce the concentric circle approximation (CCA), which gives us a starting point

for tackling the problem of devising an approximate pressure-maximizing spiral, the QOS. We also formally prove, in the CCA, the existence of a maximal pressure spiral, and we derive a functional form for the QOS based on the CCA. Section 5 compares the Archimedean and quasi-optimal spirals and presents several additional numerical results. Section 6 discusses the phenomenon of air lift and derives an approximate expression for it. We then draw conclusions and discuss some open problems in §7.

2. Preliminaries

(a) Assumptions

To model the Wirtz pump, which we assume to consist of a slow-turning spiral of pipe in a vertical plane, the pipe containing alternating plugs of water and air, we need to make several assumptions, which we now list and comment upon. We name the assumptions where we need to refer to them again.

(i) *The plug assumption.* This is the main assumption and without at least some version of it, it would be unclear how to model the pump. The assumption is that the plugs of water move within the pipe but remain intact, that is, they remain as single plugs and no air passes through them, no matter how the pipe is orientated. Several parameters (in particular, the pipe inner diameter and the surface tension and viscosity of water) affect the validity of this assumption. A video of an experimental helical pump can be found at [10], which shows that the plug assumption appears to apply to the translucent pipe used in that case.

(ii) *Pascal's Law.* The pressure difference, Δp, between two points a vertical distance Δh apart in an incompressible, stationary fluid of density ρ_w is given by $\Delta p = \rho_w g \Delta h$, where g is the acceleration due to gravity.

(iii) *Boyle's Law* [9]. This states that, for a fixed quantity of an ideal gas at constant temperature, $pv = \text{const.}$, where p and v are the pressure and volume, respectively. The assumption that the pump is slow-turning means that the compression of air, assumed ideal, takes place at roughly constant temperature. An alternative to Boyle's Law, the adiabatic equation, $pv^\gamma = \text{constant}$ [9], is used in [7], with $\gamma = 1.15$.

(iv) *Periodicity.* The arrangement of plugs looks identical after one rotation of the spiral—that is, we assume that any transient dynamical behaviour has decayed and the system is in a steady state.

(v) Air has negligible density ($\rho_{air} \sim 1\,\text{kg}\,\text{m}^{-3}$, whereas $\rho_w = 1000\,\text{kg}\,\text{m}^{-3}$).

(vi) For the conditions in the pump, an insignificant quantity of air dissolves in the water.

(vii) We make several approximations relating to the volume of spiral and helical pipes—see §2b.

We now comment briefly on these assumptions. The most important of them is the plug assumption, and its validity depends critically on the inner diameter of the pipe used. Evidence that this assumption holds for the parameters in table 1 is seen in [10], in which the inner diameter of the pipe used appears to be similar to ours. Pascal's Law is certainly valid in this situation, but it is arguable which one of Boyle's Law (constant temperature) and the adiabatic equation (no transfer of heat) better describe the compression of air here: in reality, the truth probably lies between the two (i.e. $\gamma \approx 1$). The periodicity assumption is plausible, and the negligibility of the density of air is certainly true. As the water is taken from a stream, it will be saturated with air at atmospheric pressure, but more will dissolve within the pump because the pressure there is higher. However, dissolving of air in water takes time, and the area of water exposed to air within the pump is small ($\sim 2 \times 10^{-4}\,\text{m}^2$—table 1), so this assumption is likely to hold too.

Table 1. Names, symbols and numerical values for the parameters for a practical Wirtz pump consisting of an Archimedean spiral.

name	symbol	numerical value
	universal parameter values	
acceleration due to gravity	g	$9.81\ \mathrm{m\,s^{-2}}$
standard atmospheric pressure	p_0	$1.01 \times 10^5\ \mathrm{N\,m^{-2}}$
density of water	ρ_w	$1.0 \times 10^3\ \mathrm{kg\,m^{-3}}$
density of air	ρ_{air}	$1.2\ \mathrm{kg\,m^{-3}}$
	parameter values for a practical pump	
number of turns	N	12
inner radius of pipe	r_{in}	7.6×10^{-3} m
cross-sectional area of pipe	$a = \pi r_{in}^2$	$1.82 \times 10^{-4}\ \mathrm{m^2}$
pipe outer diameter	d	2.0×10^{-2} m
archimedean spiral constant	$b = d/2\pi$	3.18×10^{-3} m
pump radius	R	0.6 m
pump parameter	$\alpha = \rho_w g R/p_0$	0.0583
air lift parameter	$\mu = \rho_w g/p_0$	$0.0971\ \mathrm{m^{-1}}$
rotation rate	—	6–8 r.p.m. (depends on stream conditions)

(b) Helices and spirals

To model the Wirtz pump, we will need an estimate of the internal volume, which we refer to from now on just as 'volume', of sections of curved pipe. It will be convenient to use polar coordinates (ρ, ψ) to define the curve taken up by the axis of the pipe, and we shall do this by specifying the radius ρ as a function of angle $\psi \geq 0$. It turns out that we will need to compute the volume contained between two angles, and also the angle given the volume. That is, we seek a function $v(\psi)$, which gives the volume between 0 and ψ, and also its inverse.

We shall concentrate mainly in this paper on pumps that consist of pipe wound into a spiral, which we define as a planar curve, described in polar coordinates by a smooth, positive, monotonically decreasing function $\rho(\psi)$, for $\psi \in \mathcal{D}$, where $\mathcal{D} = [0, \psi_{max})$ is a finite or semi-infinite subset of $\mathbb{R}$. Such a strict definition turns out to be convenient for this work. Note that our spirals move *towards* the origin as ψ increases. It is often convenient to write $\rho(\psi) = Rr(\psi)$, where R has the dimensions of length and $r(\psi)$ is a dimensionless function of ψ, with $r(0) = 1$. The special case of a helical pipe is defined by $\rho(\psi) = \text{const}$.

We observe now that, in the helical case, and in spiral cases when, for some $\psi_0 \in \mathcal{D}$, $\rho(\psi_0) - \rho(\psi_0 + 2\pi) < d$, where d is the outer diameter of the pipe, the spiral cannot be wound in a plane without the pipe intersecting itself. In such cases, we imagine it instead to be wound around an appropriate solid of revolution. The length of such a curve will, of course, differ from the planar case, but the difference is negligible provided that $\rho \gg d$. As a guide, consider a tightly wound helix in which successive turns touch. Then, approximating the actual length L of one helical turn of radius R and pitch d as the circumference $2\pi R$ of a circle of radius R gives $L/2\pi R = \sqrt{1 + d^2/4\pi^2 R^2}$. (We have approximated L as the hypotenuse of a right-angled triangle with adjacent and opposite sides of length $2\pi R$ and d, respectively.) For this to be in (relative) error by 0.1% gives $L/2\pi R = 1.001$, and for $d = 2 \times 10^{-2}$ m (table 1), we have that $R \geq 0.071$ m. In practice, all turns have considerably greater radius than this. For example, the radius of the smallest turn in figure 1 is 0.36 m.

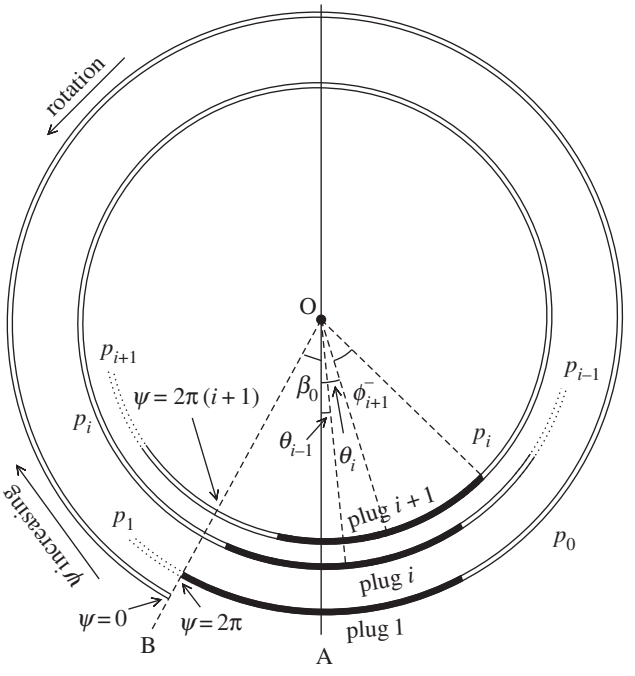

Figure 3. Pressures (p_i) and various angles used in modelling the Wirtz pump. Plugs of water are shown in black, and of air, in white.

We now make the approximation that the volume of a length of curved pipe of inner cross-sectional area a, whose axis lies along a given space curve $\mathcal{C}$, is given by $v(\psi) = a\sigma(\psi)$, where $\sigma(\psi)$ is the arc length of $\mathcal{C}$ as a function of ψ. This, too, will be a good approximation, provided that the radius of curvature of $\mathcal{C}$ is nowhere too small. We refer to this hereafter as 'the volume assumption'.

As an example of a spiral case, let us consider the Archimedean spiral, in which $\rho(\psi) = Rr(\psi) = R(1 - b\psi/R)$. Here, R, which we refer to as the pump radius, is the distance from the origin to the centreline of the pipe at $\psi = 0$, hence, as $r(\psi)$ is decreasing, R is the radius of the smallest circle, centred at the origin, that contains the centreline of the spiral; and $b \ll R$ is a positive constant (figure 3). This is the most tightly wound, strictly planar spiral possible if $b = d/2\pi$. For this spiral,

$$\sigma(\psi) = \int_0^\psi \sqrt{(R - b\xi)^2 + b^2}\,\mathrm{d}\xi = \frac{b}{2}\ln\left(\frac{R + e(0)}{R - b\psi + e(\psi)}\right) + \frac{Re(0) - (R - b\psi)e(\psi)}{2b}, \tag{2.1}$$

where $e(\psi) = \sqrt{(R - b\psi)^2 + b^2}$. For other spirals, $\sigma(\psi) = \int_0^\psi \sqrt{\rho^2 + (\mathrm{d}\rho/\mathrm{d}\xi)^2}\,\mathrm{d}\xi$ may or may not be available in closed form. Even in the Archimedean case, there is no simple expression for $\sigma^{-1}(x)$.

(c) Realistic parameters

Table 1 gives a list of realistic parameter values that apply to the Wirtz pump shown in figure 1.

3. Derivation of the mapping

As mentioned in the Introduction, we model the pump as a dynamical system: our aim is to derive a function (a mapping) that maps a pair of variables from their values in one turn of the spiral to those in the next. As we shall see, the mapping depends on two dimensionless parameters, $\phi \in [0, \pi]$ and $\alpha > 0$, both defined below.

We consider first the general spiral case $\rho(\psi) = Rr(\psi)$, and then specialize this to the helical case by setting $\rho(\psi) = R$ const. Figure 3 shows two short sections of the pipe, these being parts of the N-turn spiral that forms the Wirtz pump. Directions such as 'clockwise', 'left' and so on refer to this figure. The turns are numbered from $i = 1$ to N, with $i = 1$ corresponding to the outermost turn—this turn has an open end, the intake. Hence, in the ith turn, $\psi \in [2(i-1)\pi, 2i\pi)$.

Within the pipe, plugs of water and air are shown in black and white, respectively. The pump rotates anticlockwise about point O and the angle $\psi \in [0, 2N\pi]$ is measured clockwise from line OB. This line passes through O, the left-hand (clockwise) end of the first plug of water, plug 1, and the open end of the pipe. These three points are collinear simply because we choose to define the first turn to contain the whole of plug 1, the rest of the turn being filled with air: effectively, we define the open end of the pipe, which is at $\psi = 0$, to be collinear with the other two points. Hereafter, when we refer to a 'plug', we mean a plug of water and in figure 3, plugs 1, i and $i+1$ are shown. We assume that all the plugs have the same arc length w, which is reasonable, because we expect the amount of water collected not to change between turns of the pump. We then define angles ψ_i, $i = 1, \ldots, N$, which are the angles between line OB and the midpoint of plug i, measured clockwise along the pipe. Hence, $0 < \psi_1 < \psi_2 \cdots < \psi_N < 2N\pi$ and, importantly, these angles are *not* measured modulo 2π.

For convenience, we also introduce another set of angles θ_i, $i = 0, \ldots, N-1$, and these are measured anticlockwise from the line OA, where point A is vertically below O. They are defined such that θ_{i-1} is the angle between OA and the midpoint of plug i. Naturally, there is a relation between ψ_i and θ_{i-1}—see equation (3.2).

The angle subtended by the ith plug at O is equal to $\phi_i^- + \phi_i^+$, where ϕ_i^- and ϕ_i^+, both assumed positive, are the angles subtended by the right- and left-hand halves of the plug, respectively. The arc length of both of these half plugs is $w/2$, and so, by the definition of ψ_i, $\sigma(\psi_i + \phi_i^+) - \sigma(\psi_i) = \sigma(\psi_i) - \sigma(\psi_i - \phi_i^-) = w/2$. It is convenient to introduce a dimensionless arc length, $s(\psi)$, defined by $s(\psi) = \sigma(\psi)/R$, so $s^{-1}(x/R) = \sigma^{-1}(x)$, and in terms of this

$$s(\psi_i + \phi_i^+) - s(\psi_i) = s(\psi_i) - s(\psi_i - \phi_i^-) = \frac{w}{2R} := \phi. \tag{3.1}$$

Angles ϕ_i^+ and ϕ_i^- are not equal in general because of the spiral geometry. From the definitions above, the angle AOB is $\beta_0 := \phi_1^+ - \theta_0$, and hence, from figure 3,

$$\psi_i = 2i\pi - \beta_0 - \theta_{i-1}. \tag{3.2}$$

If l_i is the length of air between plugs i and $i+1$, with l_0 being the length of air in the first turn, then we have

$$\frac{l_i}{R} = s(\psi_{i+1} - \phi_{i+1}^-) - s(\psi_i + \phi_i^+) \quad \text{with} \quad \frac{l_0}{R} = s(2\pi) - \frac{w}{R} = s(2\pi) - 2\phi. \tag{3.3}$$

By the volume assumption, §2b, the volume of the air between the right-hand end of plug $i+1$ and the left-hand end of plug i is al_i; we write its pressure as p_i.

We now derive a pair of difference equations that together describe the hydrostatic behaviour of the Wirtz pump. Our starting point is Pascal's Law, $\Delta p = \rho_w g \Delta h$. Considering plug i in figure 3, the difference in height between its right and left ends is

$$\Delta h_i = -\rho(\psi_i - \phi_i^-)\cos(\phi_i^- + \theta_{i-1}) + \rho(\psi_i + \phi_i^+)\cos(\phi_i^+ - \theta_{i-1}) = \frac{(p_i - p_{i-1})}{\rho_w g}.$$

Hence, letting $q_i = p_i/p_0$ be the relative pressure, and using equation (3.2) to eliminate θ_{i-1}, we have

$$q_i = q_{i-1} + \alpha[r(\psi_i + \phi_i^+)\cos(\psi_i + \phi_i^+ + \beta_0) - r(\psi_i - \phi_i^-)\cos(\psi_i - \phi_i^- + \beta_0)],$$

where $\alpha = \rho_w g R/p_0$ and $r(\psi) = \rho(\psi)/R$. Finally, from equation (3.1), we have that $\psi_i + \phi_i^+ = s^{-1}(s(\psi_i) + \phi)$ and $\psi_i - \phi_i^- = s^{-1}(s(\psi_i) - \phi)$, and, using these in the above, we obtain, for $i = 1, \ldots, N$,

$$q_i = q_{i-1} + \alpha(r[s^{-1}(s(\psi_i) + \phi)] \cos[s^{-1}(s(\psi_i) + \phi) + \beta_0] - r[s^{-1}(s(\psi_i) - \phi)] \cos[s^{-1}(s(\psi_i) - \phi) + \beta_0]). \tag{3.4}$$

This equation alone is insufficient to describe the system completely. We therefore derive a second difference equation, relating angles, for which we use Boyle's Law in the form $p_i v_i = p_0 v_0$, for $i = 1, \ldots, N$, where p_0 is the ambient pressure and $v_0 = a l_0$. Hence, $l_i = l_0/q_i$, and so from equation (3.3), we have

$$s(\psi_{i+1} - \phi_{i+1}^-) - s(\psi_i + \phi_i^+) = \frac{l_0}{R q_i}.$$

Again from equation (3.1), we have that $s(\psi_i + \phi_i^+) = s(\psi_i) + \phi$; and, with i replaced by $i+1$, we also have $s(\psi_{i+1} - \phi_{i+1}^-) = s(\psi_{i+1}) - \phi$. Therefore, using equation (3.3) to eliminate l_0,

$$\psi_{i+1} = s^{-1}\left(s(\psi_i) + 2\phi + \frac{s(2\pi) - 2\phi}{q_i}\right), \quad i = 1, \ldots, N-1. \tag{3.5}$$

The operation of the pump is thus described by equations (3.4) and (3.5), which together comprise a two-dimensional, autonomous discrete dynamical system with state vector (q_i, ψ_i). The two initial conditions are q_0 and $\beta_0 = \phi_1^+ - \theta_0$, with the former always being taken to be equal to 1, because the pressure in the first turn is p_0, the ambient pressure. The system can be seen to be controlled by two dimensionless parameters, $\alpha = \rho_w g R/p_0 \in [0, \infty)$ and $\phi = w/2R \in [0, \pi]$, which is half the angle subtended at O by a plug of water of length w in a pipe bent into a circle of radius R. By definition, α can in principle be made as large as we please by increasing R; in practical terms, ϕ, which is proportional to α, can be adjusted by varying the depth of submersion of the spiral, or, more easily, by widening out the open end of the pipe into a scoop. For the practical pump, $w \approx 0.96$ m, giving $\phi \approx 0.8$.

We can also use equation (3.1) to derive the expressions for the angles $\phi_i^\pm$, should they be needed:

$$\phi_i^+ = s^{-1}(s(\psi_i) + \phi) - \psi_i \quad \text{and} \quad \phi_i^- = \psi_i - s^{-1}(s(\psi_i) - \phi). \tag{3.6}$$

To generate a set of values of (q_i, ψ_i), we need the initial conditions (q_0, β_0) and also the fact that, by definition, ψ_1 is the angle between line OB and the midpoint of plug 1 in figure 3, thus giving $\psi_1 = s^{-1}(s(2\pi) - \phi)$. This, with equation (3.2), gives $\beta_0 = 2\pi - s^{-1}(s(2\pi) - \phi) - \theta_0$. From these, we can find q_1 from equation (3.4), and, knowing q_1, we can use equation (3.5) to find ψ_2. Hence, we can now find q_2, and so on. We can thus compute (q_i, ψ_i) for all i.

Although we do not study the helical case further here, for the sake of completeness, we derive the mapping that describes it. In this case, $\rho(\psi) = R r(\psi) = R$ and $\phi_i^\pm = \phi = w/2R$ are both constants. Also, $\psi_i = 2i\pi - \phi + \theta_0 - \theta_{i-1}$, $l_0 = R(2\pi - 2\phi)$ and $\beta_0 = \phi - \theta_0$. Using these in equations (3.4) and (3.5) gives

$$\left.\begin{aligned} q_i &= q_{i-1} + 2\alpha \sin\phi \sin\theta_{i-1} \\ \text{and} \qquad \theta_i &= \theta_{i-1} + 2(\pi - \phi)\left(1 - \frac{1}{q_i}\right). \end{aligned}\right\} \tag{3.7}$$

We give some results for the mapping in the Archimedean and other spiral cases in §5.

4. An approximate pressure-maximizing spiral

(a) The concentric circle approximation and the 3 o'clock spiral

It is easy to see that the spiral that produces the maximum *peak* pressure consists of a set of N D-shaped turns connected in series, with the vertical sections being full of water and all having

length w; and the curved parts successively decreasing in length according to Boyle's Law, and being filled with air. Such a spiral would give a peak pressure, q_N, of $N\rho_w g w$ for one particular orientation of the spiral, but the pressure would be much reduced in other orientations: q_N would, in other words, be far from constant as the spiral rotates. In practice, variable pressure is undesirable, because, among other things, plugs in the delivery pipe, which takes water to the destination, would move backwards as well as forwards, thereby dissipating energy, and also, the torque required to turn the pump would vary with orientation.

We now look at a heuristic argument that leads to an approximation to a notional spiral which, for given R, w and N, gives the maximum output pressure, q_N, and, moreover, this pressure is constant as the spiral rotates. We then transform this notional spiral into an actual one, for which the output pressure is both close to maximal and close to constant. Our argument is based on an approximation and an assumption.

The approximation we name the 'concentric circle approximation' (CCA), and in it we represent the spiral as a set of N concentric circles, each centred on O, with the radius of the ith circle being $\rho_i = Rr_i$. For convenience, we refer to the resulting pipe shape as the 'CCA spiral', even though it is only notionally a spiral.

The assumption is that the angles θ_i between vertical line OA in figure 3, and the centres of the plugs, for all i, are equal to $\pi/2$, and we refer to any spiral with this configuration of plugs as a '3 o'clock spiral'. The reasoning behind this plug positioning is that, in the CCA at least, Δh_i, which is the length of the projection of each plug onto the vertical axis, is a maximum. By Pascal's Law, the difference between q_i and q_{i-1} is therefore maximized, and so q_N is maximized. This is proved rigorously in theorem 4.2.

The relative pressure in the ith turn is q_i, $i = 0, \ldots N$, with q_N being that at the high-pressure end of the Nth plug (i.e. the output pressure). As before, $q_0 = r_0 = 1$. As we have $\theta_i = \pi/2$, we can now derive recursion formulae for q_i and r_i, the latter defining the CCA spiral.

The details are as follows. The projection of the ith plug onto the vertical axis has length $\Delta h_i = 2Rr_i \sin(\phi/r_i)$, where ϕ/r_i is the angle subtended at O by half the ith plug. Pascal's Law then gives

$$q_{i+1} = q_i + 2\alpha r_i \sin\frac{\phi}{r_i}, \tag{4.1}$$

where, as before, $\alpha = \rho_w g R/p_0$ and so $2\alpha = 0.1166$.

Now consider the outermost turn, $i = 0$, which has scaled radius $r_0 = 1$. Letting l_i be the length of the air plug in turn i, we have $l_0 = 2\pi R - w$. Boyle's Law then gives $l_i = l_0/q_i$. Now, from the circumference of the ith turn, we find that $l_i + w = 2\pi R r_i = l_0/q_i + w$, and hence, with $r_\infty = \phi/\pi = w/2\pi R$, we find

$$r_i = \frac{1 - r_\infty}{q_i} + r_\infty. \tag{4.2}$$

Equations (4.1) and (4.2) together allow us to compute, respectively, the relative pressures and the radii of successive turns in the concentric circle approximation to the pressure-maximizing spiral, given the parameter values and the fact that $q_0 = 1$. Assuming fixed R and N, the only free parameter is $\phi = w/2R$. Two natural questions then arise: (i) is there an arrangement of plugs that gives a higher output pressure, q_N, than that of the 3 o'clock spiral? and (ii) does there exist a value of ϕ, ϕ^* say, that, given that $\theta_i = \pi/2$ for all i, results in a maximum q_N? We examine the first of these questions in the next section.

(b) Proof of output pressure maximality

The derivation of the following system is as in §4a, but with the $\theta_i = \pi/2$ replaced by $\theta_i = \pi/2 + \eta_i$. The variables $\eta_1, \eta_2, \ldots, \eta_N$ measure the deviation from a 3 o'clock spiral. In non-dimensional variables r_i and q_i, equation (4.1) becomes $q_{i+1} = q_i + 2\alpha\phi\,\mathrm{sinc}(\phi/r_i)\cos\eta_{i+1}$ for $i = 0, \ldots, N-1$. Here, sinc denotes the function $\mathrm{sinc}\, s := \sin s/s$ with its singularity at $s = 0$ removed. Note that q_1 depends only on η_1, q_2 only on η_1 and η_2, and so on.

Additionally, as $r_i = (1 - r_\infty)/q_i + r_\infty$, the dependence of r_i on $\eta_1, \eta_2, \ldots, \eta_i$ is implicit in the dependence of q_i on those variables.

Lemma 4.1. *Let $r_\infty = \phi/\pi < 1$ and define, for $r_\infty < r \le 1$, the function*

$$Z(r) = \frac{1 - r_\infty}{r - r_\infty} + 2\alpha\phi \operatorname{sinc}\left(\frac{\phi}{r}\right).$$

In addition, for each $v \ge 1$, define

$$d(v) = Z\left(\frac{1 - r_\infty}{v} + r_\infty\right).$$

Then, provided that $2\alpha\pi(1 - r_\infty) \le 1$, $Z(r)$ is decreasing on $r_\infty < r \le 1$ and $d(v)$ is increasing for $v \ge 1$.

Proof. We calculate

$$Z'(r) := \frac{\mathrm{d}Z}{\mathrm{d}r} = -\frac{1 - r_\infty}{(r - r_\infty)^2} + 2\alpha\left(\sin\left(\frac{\phi}{r}\right) - \left(\frac{\phi}{r}\right)\cos\left(\frac{\phi}{r}\right)\right). \tag{4.3}$$

As $\phi/r < \pi$ and the function $u \mapsto \sin u - u\cos u$ is increasing for $0 \le u \le \pi$, an upper bound for the rightmost term in (4.3) is $2\alpha\pi$. The leftmost term is bounded above by $-(1 - r_\infty)^{-1}$, so that $Z'(r) \le 0$, provided $-(1 - r_\infty)^{-1} + 2\alpha\pi \le 0$. The latter easily rearranges to the condition in the statement of the lemma.

Let us now assume that this condition holds. That d as defined is increasing is now easy to see. Indeed,

$$v^2 d'(v) = -(1 - r_\infty)Z'\left(\frac{1 - r_\infty}{v} + r_\infty\right),$$

where the argument, a, say, of Z' on the right lies between r_∞ and 1 and hence, by the previous part of the proof, $Z'(a) \le 0$. Thus $d'(v) \ge 0$. Alternatively, simply note that, for $v_1 \ge v_2 \ge 1$, we have

$$r_\infty \le \frac{1 - r_\infty}{v_1} + r_\infty \le \frac{1 - r_\infty}{v_2} + r_\infty \le 1,$$

and hence, as Z is decreasing, we obtain $d(v_1) \ge d(v_2)$. ∎

The next result shows that, within the class of CCA spirals, the maximum relative output pressure is uniquely attained by the so-called 3 o'clock spiral. The proof is shortened somewhat by the following conventions. Firstly, by r_i we mean $r_i = r_i(\eta_1, \ldots, \eta_i)$ and $\eta^{(i)} = (\eta_1, \ldots, \eta_i)$ will denote the argument of r_i. The same convention will apply to each q_i. A natural consequence of this notation is that $r_i(\eta^{(i-1)}, 0)$ will denote r_i evaluated at the i-tuple $(\eta_1, \ldots, \eta_{i-1}, 0)$, and also that the i-tuple consisting of i entries of 0 is written $0^{(i)}$.

Theorem 4.2. *In the system*

$$q_{i+1} = q_i + 2\alpha\phi \operatorname{sinc}\left(\frac{\phi}{r_i}\right)\cos\eta_{i+1} \quad i = 0, \ldots, N - 1$$

$$r_i = \frac{1}{q_i}(1 - r_\infty) + r_\infty \quad i = 0, \ldots, N$$

with $r_0 = q_0 = 1$, and provided that $2\alpha\pi(1 - r_\infty) \le 1$, it holds that

$$q_N(\eta^{(N)}) \le q_N(0^{(N)}), \tag{4.4}$$

with equality if and only if $\eta_i = 0$ for $i = 0, \ldots, N$.

Proof. First note that

$$q_N = q_{N-1} + 2\alpha\phi \operatorname{sinc}\left(\frac{\phi}{r_{N-1}}\right)\cos\eta_N \le q_{N-1} + 2\alpha\phi \operatorname{sinc}\left(\frac{\phi}{r_{N-1}}\right).$$

By rearranging (4.2), we can write $q_{N-1} = (1 - r_\infty)/(r_{N-1} - r_\infty)$, so that

$$q_N \le \frac{1 - r_\infty}{r_{N-1} - r_\infty} + 2\alpha\phi \operatorname{sinc}\left(\frac{\phi}{r_{N-1}}\right) \tag{4.5}$$

$$= Z(r_{N-1}). \tag{4.6}$$

For later use, we record the fact that $Z(r_{N-1}) = q_N(\eta^{(N-1)}, 0)$.

Now note that $r_{N-1}(\eta^{(N-2)}, 0) \le r_{N-1}$, which is true because q_{N-1} is maximized when $\eta_{N-1} = 0$, so that by applying lemma 4.1, it follows that $Z(r_{N-1}) \le Z(r_{N-1}(\eta^{(N-2)}, 0))$. Next, note that

$$r_{N-1}(\eta^{(N-2)}, 0) = \frac{1 - r_\infty}{q_{N-2} + 2\alpha\phi \operatorname{sinc}(\phi/r_{N-2})} + r_\infty \tag{4.7}$$

$$= \frac{1 - r_\infty}{Z(r_{N-2})} + r_\infty. \tag{4.8}$$

Hence $Z(r_{N-1}) \le Z((1 - r_\infty)/Z(r_{N-2}) + r_\infty) = d(Z(r_{N-2}))$. Note that $q_N(\eta^{(N-2)}, 0, 0) = d(Z(r_{N-2}))$.

Now $r_{N-2}(\eta^{(N-3)}, 0) \le r_{N-2}$, because q_{N-2} is maximized when $\eta_{N-2} = 0$, and hence (again applying lemma 4.1) $Z(r_{N-2}) \le Z(r_{N-2}(\eta^{(N-3)}, 0))$. As both sides of the latter inequality are larger than 1 (each being a possible value of the relative pressure q_{N-1}), lemma 4.1 again applies, and we must have

$$d(Z(r_{N-2})) \le d(Z(r_{N-2}(\eta^{(N-3)}, 0))).$$

Drawing the preceding steps together gives

$$Z(r_{N-1}) \le d(Z(r_{N-2})) \le d(Z(r_{N-2}(\eta^{(N-3)}, 0))). \tag{4.9}$$

Now one can replace $r_{N-2}(\eta^{(N-3)}, 0)$ with an expression like the one in (4.7) but with $N - 3$ in place of $N - 2$, and then repeat the argument above to obtain $d(Z(r_{N-2}(\eta^{(N-3)}, 0))) = d(d(Z(r_{N-3})))$. Coupling this with (4.9) gives

$$Z(r_{N-1}) \le d(Z(r_{N-2})) \le d(d(Z(r_{N-3}))), \tag{4.10}$$

which, when iterated, yields

$$Z(r_{N-1}) \le d^{(j-1)}(Z(r_{N-j})) \tag{4.11}$$

for $j = 1, 2, \ldots, N$. Here, $d^{(j-1)}(s)$ represents the map d applied $j - 1$ times to s. At each stage, the construction gives us

$$q_N(\eta^{(N-j)}, 0^{(j)}) = d^{(j-1)}(Z(r_{N-j})). \tag{4.12}$$

Using (4.12), (4.6) and (4.11) gives $q_N \le d^{(N-1)}(Z(r_0)) = q_N(0^{(N)})$, which concludes the proof of (4.4).

To see that $q_N < q_N(0^{(N)})$ with equality if and only if $\eta_i = 0$ for $i = 1, \ldots, N$, first note that Z is strictly decreasing on $(r_\infty, 1]$, as can be seen by looking at the condition required for $Z'(r) = 0$ in the proof of lemma 4.1. It follows from this that each inequality

$$Z(r_{N-j}) \le Z\left(\frac{1 - r_\infty}{Z(r_{N-j-1})} + r_\infty\right),$$

holds strictly unless $\eta_{N-j} = 0$ for each $1 \le j \le N - 1$. From the first line of the proof we also know that $q_N = Z(r_{N-1})$ only if $\eta_N = 0$. Hence q_N is uniquely maximized when $\eta_1 = \cdots \eta_N = 0$. ∎

We point out that the optimal spiral calculation applies provided that ϕ is such that $2\alpha(\pi - \phi) \le 1$. In our case, this holds for all $\phi \in [0, \pi]$ because $2\alpha\pi \sim 0.3663$. Thus, the 'optimal spiral' would be the 3 o'clock spiral with $\phi = \phi^*$ as in §4a. We also remark that the 3 o'clock spiral is a global pressure maximizer regardless of the initial conditions.

(c) The quasi-optimal spiral

Clearly, the CCA proposed in §4a does not even give a spiral—it gives instead a set of unconnected concentric circles of pipe, with the property that, were these circular pipes somehow connected together in order of decreasing radius, the output pressure q_N would be a maximum. In this section, we describe an interpolation scheme that turns the optimal CCA spiral into a true spiral, which we refer to as the 'quasi-optimal spiral' (QOS), and which we assume produces an output pressure which is 'close to maximal'. Specifically, we seek a smooth, monotonically decreasing function, $r(\psi)$, such that $r(2i\pi) \approx r_i$, $i = 0, \ldots N$, with r_i being given by equations (4.1) and (4.2). We then use this $r(\psi)$ to compute the output pressure numerically, using the mapping, equations (3.4), (3.5), as set out in §3.

We take the following heuristic approach, starting from equations (4.1) and (4.2). With $r_\infty = \phi/\pi$, equation (4.2) gives $q_i = (1 - r_\infty)/(r_i - r_\infty)$. Furthermore, defining $x_i = r_i - r_\infty$, equation (4.1) gives

$$x_{i+1} = F(x_i) = \frac{x_i}{1 + \gamma x_i(x_i + r_\infty)\sin(\pi/(1 + x_i/r_\infty))} = x_i - \gamma\pi x_i^3 + O(x_i^5), \tag{4.13}$$

where $\gamma = 2\alpha/(1 - r_\infty) > 0$. Making the ansatz $x_i = (2\gamma\pi i + x_0^{-2})^{-1/2}$, we find, for large i, the following asymptotic expansion:

$$x_{i+1} - x_i + \gamma\pi x_i^3 \sim \frac{3}{16}\sqrt{\frac{2}{\gamma\pi}}\, i^{-5/2} + O(i^{-7/2}),$$

terms of order $i^{-1/2}$ and $i^{-3/2}$ cancelling out. What is important here is that the above is consistent with x_i tending to zero as $i^{-1/2}$ for large i. This suggests that we model the required smooth $r(\psi)$, which interpolates the r_i values, by

$$r(\psi) = (1 - r_\infty)\sqrt{\frac{1 + b_1\psi + \cdots + b_{D-1}\psi^{D-1}}{1 + a_1\psi + \cdots + a_D\psi^D}} + r_\infty = (1 - r_\infty)\sqrt{\frac{B(\psi)}{A(\psi)}} + r_\infty, \tag{4.14}$$

for suitable D and constants $a_1, \ldots, a_D$ and $b_1, \ldots b_{D-1}$, this expression giving $r(0) = 1$ and tending to r_∞ as $\psi^{-1/2}$ for large ψ, as the above suggests it should. Other possibilities for $r(\psi)$ could be considered, but for the practical parameter values, this model works remarkably well, even (especially) for $D = 2$—see below.

Now we have a suitable $r(\psi)$, we can compute scaled arc lengths $s(\psi)$ by $s(\psi) = \int_0^\psi \sqrt{r^2 + (\mathrm{d}r/\mathrm{d}t)^2}\,\mathrm{d}t$. The inversion of this requires a numerical algorithm, and the following, based on Newton–Raphson [11], is effective for such a problem.

Inversion Algorithm. Let $h(x) > 0$ for $x \geq 0$ be a positive, monotonically decreasing function of x, and let $S = \int_0^\psi h(x)dx$, with $S_\infty = \int_0^\infty h(x)dx$. Then the following iterative scheme can be used to find $\psi = \lim_{i\to\infty}\psi_i$, given $S \in [0, S_\infty)$:

$$\psi_{i+1} = \psi_i + \frac{\xi_i}{h(\psi_i)}, \quad \xi_{i+1} = \xi_i - \int_{\psi_i}^{\psi i+1} h(x)\,\mathrm{d}x \quad \text{with } \psi_0 = 0,\ \xi_0 = S.$$

This is derived from the Newton–Raphson iteration for solving $f(\psi) = 0$ for ψ, in which an improved estimate of the solution, ψ_{i+1}, is computed from ψ_i via $\psi_{i+1} = \psi_i - f(\psi_i)/f'(\psi_i)$. For our problem, $f(\psi) = \int_0^\psi h(x)\,\mathrm{d}x - S$, and therefore $f'(\psi) = h(\psi)$. Defining $\xi_i = S - \int_0^{\psi_i} h(x)\,\mathrm{d}x$, we have that $\xi_{i+1} = \xi_i - \int_{\psi_i}^{\psi_{i+1}} h(x)\,\mathrm{d}x$. This is one half of the algorithm. Applying Newton–Raphson directly to the problem $f(\psi) = 0$, we have

$$\psi_{i+1} = \psi_i - \frac{1}{h(\psi_i)}\left(\int_0^{\psi_i} h(x)\,\mathrm{d}x - S\right) = \psi_i + \frac{\xi_i}{h(\psi_i)},$$

which gives the other half of the algorithm. By definition, $\psi_0 = 0$ implies that $\xi_0 = S$, and we take these as our initial conditions. This completes the derivation.

In this form, the algorithm is efficient: not only is it quadratically convergent close to the solution, but the range of the integral to compute ξ_{i+1} from ξ_i shrinks with increasing i, and this is advantageous given that this integral will usually need to be computed numerically.

5. Numerical results

(a) The Archimedean spiral

We simulate the behaviour of a pump consisting of an Archimedean spiral using equations (3.4) and (3.5), with $s(\psi) = \int_0^\psi \sqrt{r^2 + (\mathrm{d}r/\mathrm{d}t)^2}\,\mathrm{d}t$, where $r(t) = 1 - bt/R$. In figure 4, several results are given for $N = 12$. On the left, we show a plot of the maximum output pressure, $q_N(\phi) = \max_{\theta_0 \in [-\pi,\pi]} q_N(\theta_0, \phi)$ as a function of ϕ. We have taken the spiral to consist of exactly 12 turns, and have computed the output pressure for only as many complete plugs as fit into this spiral: if the last plug were to project beyond the end of the spiral by even a small amount, this plug is discounted, and the last turn is assumed to be filled with air. This number of whole plugs is shown on the figure, which makes an important point: by varying θ_0, and thereby changing the configuration of the plugs, any output pressure between 1 and the maximum possible can be produced. This justifies our claim that the pump is self-regulating because it will automatically choose a configuration to deliver the required output pressure, provided that this is no more than the maximum possible.

The middle and right figures apply to the situation when $\phi = \phi^* = 1.27$, giving $q_{12}^* = 1.93$, the maximum pressure. The middle figure shows the deviations from a 3 o'clock spiral, η_i, in the Archimedean case, and on the right we show the configuration of plugs for the maximum pressure. The latter two figures should be contrasted with their counterparts in the quasi-optimal case shown in figure 6.

(b) The CCA and quasi-optimal spirals

It is straightforward to investigate the performance of the CCA spiral. Using equations (4.1) and (4.2), we fix $R = 0.6$ and compute q_i, r_i, $i = 0, \ldots, 12$ for a range of values of ϕ. From this, we estimate ϕ^* and q_N^*. With $\alpha = 0.0583$, we find $\phi^* = 1.38$ and $q_N(\phi^*) = 2.12$ (figure 5).

We now show numerically how the discussion of a QOS in §4c works out in practice. The approach is as follows: first, we use equation (4.13) in the form $r_{i+1} = r_\infty + F(r_i - r_\infty)$, with $r_0 = 1$, to find r_i, $i = 1, \ldots, N$—this is the same as using equations (4.1) and (4.2). Then, for a reason given later in this section, we fix $D = 2$ in equation (4.14), and use the method of least squares to find the coefficients in polynomials $A(\psi) = 1 + a_1\psi + a_2\psi^2$ and $B(\psi) = 1 + b_1\psi$. This requires the minimization of

$$K(a_1, a_2, b_1) = \sum_{i=0}^{N} [(r_i - r_\infty)^2 A(2i\pi) - (1 - r_\infty)^2 B(2i\pi)]^2,$$

with respect to a_1, a_2 and b_1. Differentiating K with respect to each of these parameters and setting the result equal to zero gives three linear equations that can be solved for a_1, a_2 and b_1. As $r_\infty = \phi/\pi$ depends on ϕ, note that a_1, a_2 and b_1 must be recomputed every time ϕ is changed. In the QOS, we find that $\phi^* = 1.36$ and $q_{12}(\phi^*) = 2.07$ (figure 5). These figures should be compared with $\phi^* = 1.38$ and $q_{12}(\phi^*) = 2.12$ in the CCA case.

For $\phi = \phi^*$, $r(\psi)$ is given approximately by

$$r(\psi) = 0.5674752\sqrt{\frac{1 + 0.008260839\psi}{1 + 0.04544979\psi + 5.037703 \times 10^{-4}\psi^2}} + 0.4325248, \tag{5.1}$$

and this gives $r(2k\pi) - r_k \in [-3.5 \times 10^{-5},\ 0.79 \times 10^{-5}]$ for $k = 0, \ldots, 12$, with the most negative error occurring for $i = 1$ and the most positive, for $i = 5$. The overall pipe length, $s(24\pi) = 36.4$ m.

The value $D = 2$ is actually suggested by the least-squares procedure just described. For the realistic parameter values at least, it often happens that, for $D > 2$, both $A(\psi)$ and $B(\psi)$ contain,

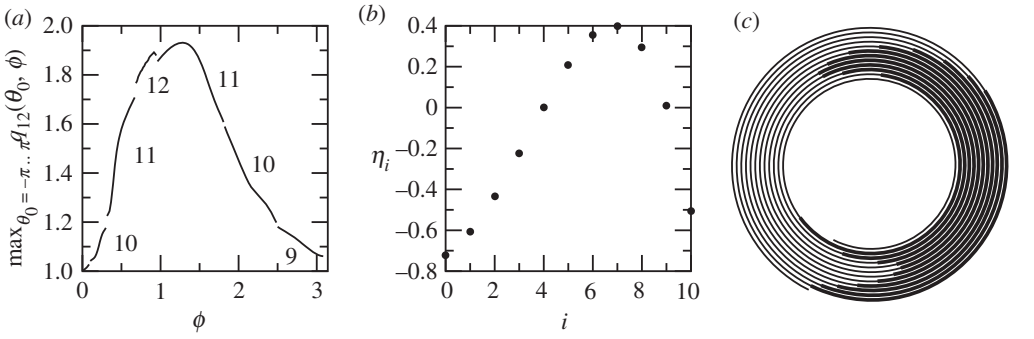

Figure 4. (*a*) Maximum output pressure for given ϕ, $q_N(\phi) = \max_{\theta_0 \in [-\pi,\pi]} q_N(\theta_0, \phi)$, for an Archimedean spiral with $N = 12$ turns. The numbers show how many whole plugs fit into the 12-turn spiral for the given pressures. The maximum pressure is $q_{12}^* = 1.93$ and occurs at $\phi = \phi^* = 1.27$. (*b*) Angles $\eta_i = \theta_i - \pi/2$ from the horizontal to the plug centres versus turn number, i, for $\phi = \phi^*$. (*c*) Configuration of the 11 water plugs (thick lines) at maximum pressure.

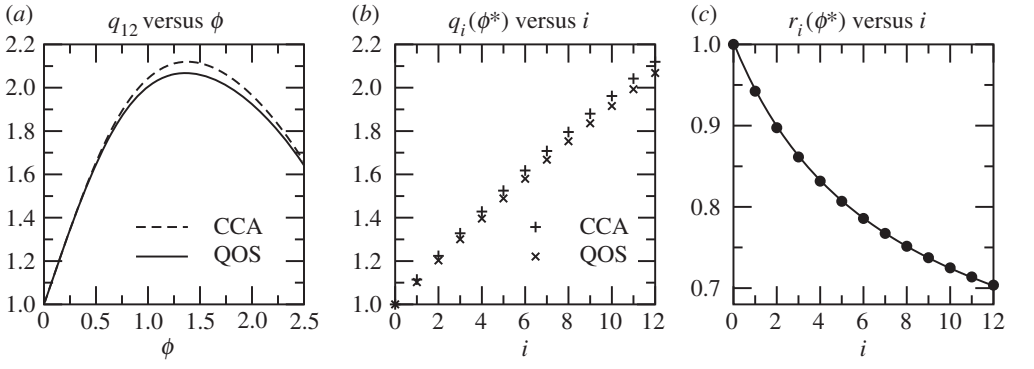

Figure 5. Comparisons of the CCA spiral and its smooth approximation, the QOS. Parameters are from table 1. In the QOS case, there are always 12 plugs of water. (*a*) q_{12} versus ϕ using the CCA (dashed line) and QOS (solid line). (*b*) Relative pressures in each turn for ϕ^*, the value of ϕ that maximizes q_{12}; CCA(+) and QOS (×). (*c*) The radius of each turn in the CCA for $\phi = \phi^*$ (filled circles) and the interpolated $r(\psi)$ from equation (5.1), (solid line).

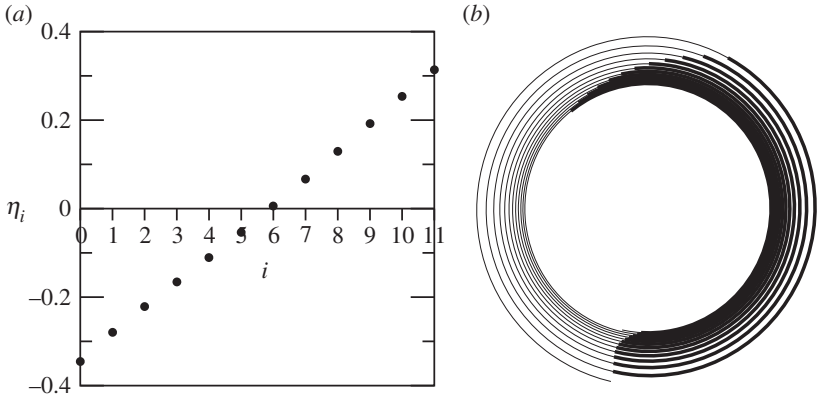

Figure 6. Behaviour of a smooth 12-turn, quasi-optimal spiral. (*a*) $\eta_i = \theta_i - \pi/2$ versus i. (*b*) The position of the plugs (thick arcs) in the pipe (thin curve), in this smooth spiral, when the maximum pressure, $q_{12} = 2.07$, is achieved. This occurs for $\phi = \phi^* = 1.36$.

approximately, a common factor, by which we mean that $A(\psi)$, $B(\psi)$ have a factor of the form $(a-\psi)$, $(b-\psi)$, respectively, with $a \approx b$. (This is a numerical calculation, so we naturally do not find $a = b$ exactly.) This is not observed when $D = 2$ however, indicating that this is a good choice for D.

In the smooth case, we no longer have that $\theta_i = \pi/2$ for $i = 0, \ldots, N-1$—see figure 6 for a plot of $\eta_i = \theta_i - \pi/2$ versus i, as well as a plot of the spiral and the plugs of water.

6. Air lift and the delivery pipe

As the output from the pump consists of alternating plugs of water and air, it is also useful to consider the behaviour of the delivery pipe—that is, the pipe connecting the pump to the destination. Clearly, there will be alternating plugs of water and air in the delivery pipe too, and so the height pumped to, ΔH, will be greater for a given pump pressure than if the delivery pipe were full of water only. This additional height gain is known as 'air lift' [1] and we estimate it here in the simple case that the delivery pipe is straight, of length L, making an angle Ω with the horizontal (figure 7). In this section, it makes more sense to use actual arc length σ rather than rescaled arclength $s = \sigma/R$.

Our objective here is to give an idea of the size of the air lift effect, and in order to do this, we model the delivery pipe as shown in figure 7. We do this in the rather restricted way implied in the figure, with its length L being *exactly* the length of M plugs of air and water, even though it makes no difference to the pressures if the length of the highest plug of air differs from l_0. We again make the assumptions set out in §2a.

It is convenient to define the air lift parameter $\mu = \rho_w g/p_0 = \alpha/R\,(\mathrm{m}^{-1})$. Pascal's Law then gives $q_{i+1} = q_i + \mu w \sin\Omega$, so that

$$q_i = 1 + i\mu w \sin\Omega, \quad i = 0, \ldots, M. \tag{6.1}$$

Boyle's Law relates lengths of air plugs to pressures, and as $q_0 = 1$, we have, as before, that $l_i = l_0/q_i$. Finally, considering the arc lengths σ_i, we have $\sigma_0 = l_0$, $\sigma_1 = w + l_0 + l_1$, and in general, using equation (6.1) and Boyle's Law, we find

$$\sigma_i = iw + l_0 \sum_{j=0}^{i} \frac{1}{1 + j\mu w \sin\Omega}. \tag{6.2}$$

In this restricted model, we assume that l_0 and w are defined by the pump, and hence are fixed. We then compute the possible values of ΔH as follows:

(i) Choose Q, the input pressure to the delivery pipe, with $Q \in [1, q_{\max}]$, where $q_{\max}$ is the maximum possible output pressure from the pump for the given w.
(ii) From equation (6.1), $Q = q_M = 1 + M\mu w \sin\Omega$. Define $M_0 = \lceil (Q-1)/\mu w \rceil$ and choose an integer $M \geq M_0$; for such a choice of M, $0 \leq \sin\Omega = (Q-1)/M\mu w \leq 1$ defines Ω.
(iii) Then, from figure 7 and equation (6.2), we have $L = \sigma_{M-1} + w = Mw + l_0 \sum_{j=0}^{M-1} (1 + j\mu w \sin\Omega)^{-1}$.
(iv) Finally, as $\Delta H(M) = L \sin\Omega$, we have, after simplification, that

$$\Delta H(M) = \frac{Q-1}{\mu}\left[1 + \frac{l_0}{w}\sum_{j=0}^{M-1}\frac{1}{M + j(Q-1)}\right]. \tag{6.3}$$

The first term in equation (6.3) is just Pascal's Law for a vertical column of water of height $Mw \sin\Omega$; the second term is the air lift. With the expression for air lift in this form, it is

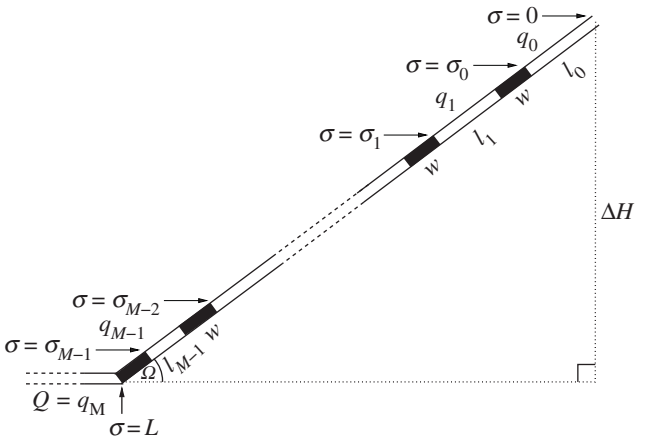

Figure 7. A delivery pipe containing M plugs of water (black) alternating with M plugs of air (white), with relative air pressures $q_0, \ldots, q_{M-1}$. The length of the pipe is L and over its length it rises by a distance ΔH; it makes an angle Ω with the horizontal. The arc length from the top of the pipe to the upper end of plug i, $i = 0, \ldots, M-1$, is σ_i and the relative pressure at the bottom of the pipe is $Q = q_M$.

unclear how ΔH varies with M. Therefore, we approximate this expression by means of the Euler–Maclaurin summation formula [11]. This states that

$$\sum_{j=0}^{M-1} f(j) = \int_0^M f(j)\,\mathrm{d}j + \frac{1}{2}[f(0) - f(M)] + \frac{1}{12}[f'(M) - f'(0)] + O(f'''(M)),$$

and letting $f(j) = [M + j(Q-1)]^{-1}$, we have

$$\sum_{j=0}^{M-1} f(j) = \frac{1}{Q-1}\ln Q + \frac{1}{2}\left[\frac{1}{M} - \frac{1}{MQ}\right] - \frac{Q-1}{12}\left[\frac{1}{M^2Q^2} - \frac{1}{M^2}\right] + O(M^{-4}).$$

For large M, we then find

$$\sum_{j=0}^{M-1} f(j) = \frac{\ln Q}{Q-1} + \frac{Q-1}{2MQ} + O(M^{-2}).$$

This expression gives a good approximation for the practical parameter values in table 1. For instance, fixing $M = 10$ we have, for $Q = 1.5$, that the sum is 0.8278, whereas the Euler–Maclaurin formula gives 0.8276; for $Q = 2.0$, the sum is 0.7188 and the approximation is 0.7181.

Hence, finally, we obtain

$$\Delta H(M) = \frac{Q-1}{\mu}\left[1 + \frac{l_0}{w}\left(\frac{\ln Q}{Q-1} + \frac{Q-1}{2MQ}\right) + O(M^{-2})\right]. \tag{6.4}$$

It now becomes clear that to maximize ΔH for fixed Q, l_0 and w, we should choose the minimal value of $M = M_0 = \lceil (Q-1)/\mu w \rceil$. For the maximal pressure Archimedean spiral considered earlier, this gives $M_0 = 7$ so that $\Delta H = 19.8\,\mathrm{m}$, of which 10.2 m, slightly more than half, is attributable to air lift. Note also that $\Delta H(M)$ varies little with M—even $\lim_{M\to\infty} \Delta H(M) = 19.3\,\mathrm{m}$.

7. Conclusion and further work

We have derived a model to describe the steady-state, hydrostatic behaviour of the Wirtz pump, which essentially consists of a spiral of pipe rotating in a vertical plane, the pipe being filled with alternating plugs of air and water. The model is a two-dimensional nonlinear mapping that relates

the positions of plugs of water, and the air pressures, in two successive turns. This model is good for a large class of spirals.

Several interesting questions concerning the pump have been considered, among them: how the pump self-regulates, automatically producing the required output pressure; how the phenomenon of air lift significantly increases (doubles, in our example) the height to which water can be pumped; and the design of a spiral that produces the maximal pressure, which varies as little as possible as the spiral rotates, for given constraints. The last question has only been partially answered. From a mathematical point of view, we have constructed a spiral that is close to optimal in both the pressure and, intuitively, the constancy senses, but the derivation of a true optimal spiral requires—and merits—further work.

This paper takes a purely hydrostatic approach and we have not studied the dynamics of the pump. For instance, how the output pressure varies during one rotation of the spiral depends critically on the function $\rho(\psi)$, which defines the spiral, and will be important in the optimization problem mentioned above. A variational approach to solving this could be considered. It is possible to describe the output pressure of a spiral in terms of an integral functional, which, to an extent, conforms to existing theory in the calculus of variations, but which also contains some novelties. Coupling such a model to one that penalizes variation in the output pressure during a rotation would be a natural next step, the results of which are not easy to anticipate.

Also of interest are how the torque required to rotate the pump varies with the configuration of the plugs of water, and the phenomenon of 'blowback'. The latter happens when the output pressure requirement is too high. The water in the intake is then ejected at high speed as the rest of the plugs rearrange themselves into a lower energy configuration—energy here being the potential energy of the plugs of water, plus that stored in the compressed air between the plugs.

As stated in §2a, the validity of our model rests on that of the plug assumption. A most worthwhile experiment would be to build a Wirtz pump from transparent pipe, which would then make it possible to see directly whether this is valid, as well as making visible the configuration of the plugs of water as conditions vary. Although the pump has been known since the mid-eighteenth century, or possibly much earlier, and the physics used in our description of it dates from the seventeenth century, only comparatively recently has the computational technology become available to enable the fast and accurate calculation of arc lengths that is needed in order to model it.

Data accessibility. This article has no supporting data.

Authors' contributions. Both authors contributed equally in formulating, carrying out and writing up the results of this research. The final version has been approved by both authors for publication.

Competing interests. We have no competing interests.

Funding. No funding has been received for this article.

Acknowledgements. The first author thanks Richard Waters for being endlessly generous with his time and practical expertise during the construction of a working Wirtz pump.

References

1. Tailer P. 1990 The spiral pump. (http://lurkertech.com/water/pump/tailer/).
2. Gregory O. 1815 *A treatise of mechanics, theoretical, practical, and descriptive*, vol. II. London, UK. (https://tinyurl.com/z25pv5y).
3. Rees A. 1820 *The Cyclopædia; or, universal dictionary of arts, sciences, and literature*, vol. XXXIII, American edition. Philadelphia, PA. (https://tinyurl.com/zvsdhmm)
4. Ewbank T. 1845 *A descriptive and historical account of hydraulic and other machines for raising water, ancient and modern, including the progressive development of the steam engine*. New York, NY. (https://archive.org/details/descriptivehisto00ewba).
5. Stuckey AT, Wilson EM. 1981 The stream-powered manometric pump. In *Proc. of the Institute of Civil Engineers Conf. on Appropriate Technology in Civil Engineering*, pp. 135–138. London, UK: ICE.

6. Mortimer GH, Annable R. 1984 The coil pump—theory and practice. *J. Hydraul. Res.* **22**, 9–22. (doi:10.1080/00221688409499408)
7. Mortimer GH. 1988 The coil pumps. PhD thesis, University of Loughborough, Loughborough, UK. (https://tinyurl.com/zhm2cwg).
8. Belcher AE. 1990 The rotary scroll collector. *Northern Eng.* **22**, 27–33.
9. Pippard AB. 1957 *Elements of classical thermodynamics*, 1st edn. London, UK: Cambridge University Press.
10. Jospa video. 2009 (http://personal.maths.surrey.ac.uk/st/J.Deane/jospa.html).
11. Abramowitz M, Stegun IA (eds). 1972 *Handbook of mathematical functions*. New York, NY: Dover Publications Inc.